Supplemental Materials

Molecular Biology of the Cell

Brown *et al*.

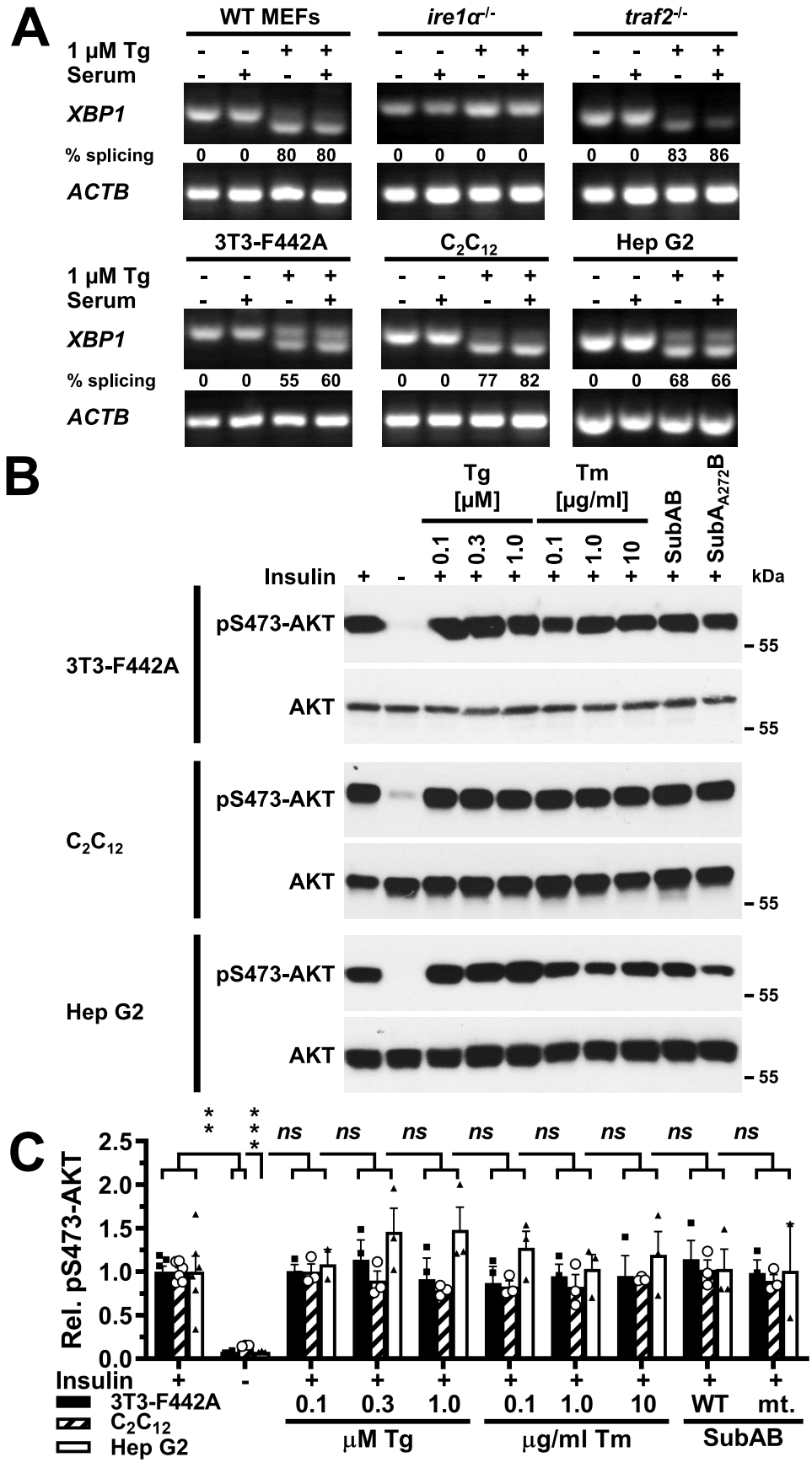
A
WT MEFs
ire1α-/-
traf2-/-
1 μM Tg
Serum
XBP1
% splicing
0 0 80 80
0 0 0 0
0 0 83 86
ACTB
3T3-F442A
C2C12
Hep G2
0 0 55 60
0 0 77 82
0 0 68 66
B
Tg [μM]
Tm [μg/ml]
+ SubAB
+ SubAA272B
Insulin
kDa
pS473-AKT
AKT
3T3-F442A
C2C12
Hep G2
55
C
Rel. pS473-AKT
ns
0.1 0.3 1.0 0.1 1.0 10 WT mt.
μM Tg
μg/ml Tm
SubAB

Figure S1

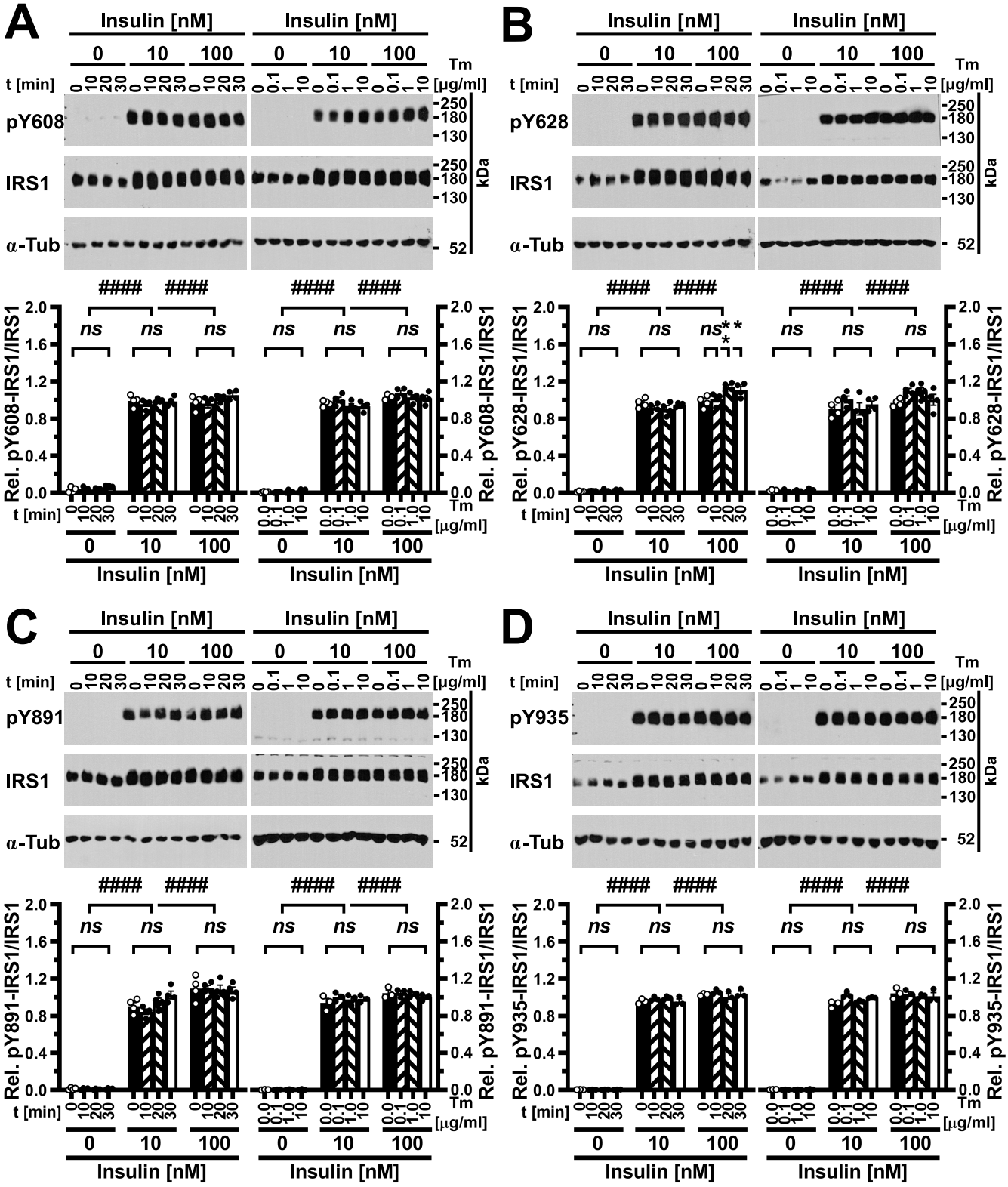
A
B
C
D
Insulin [nM]
0
10
100
t [min]
Tm
[µg/ml]
pY608
pY628
pY891
pY935
IRS1
α-Tub
kDa
250
180
130
52
Rel. pY608-IRS1/IRS1
Rel. pY628-IRS1/IRS1
Rel. pY891-IRS1/IRS1
Rel. pY935-IRS1/IRS1
####
ns
**
*

Figure S2

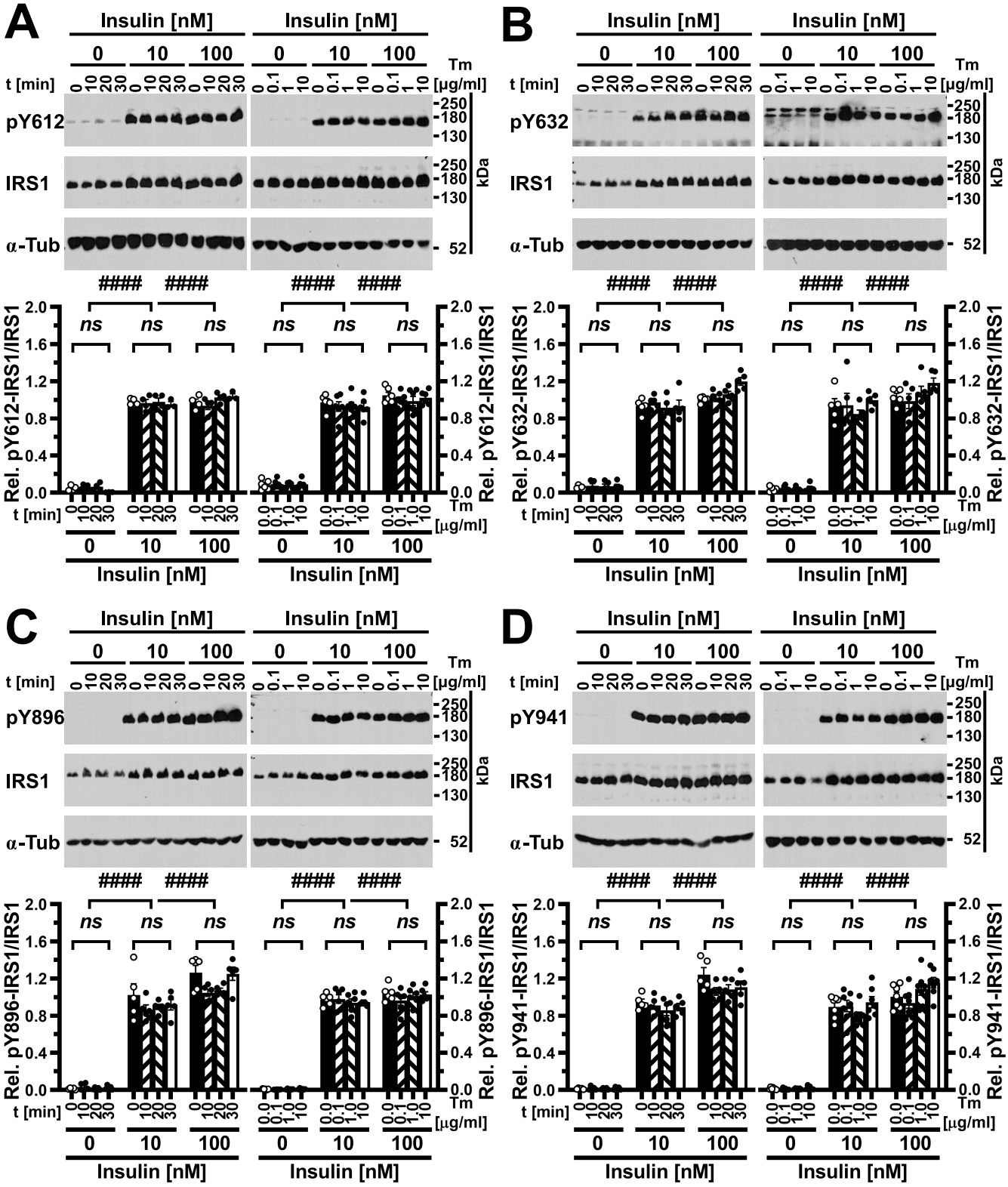
A
B
C
D
Insulin [nM]
0
10
100
t [min]
Tm
[µg/ml]
pY612
pY632
pY896
pY941
IRS1
α-Tub
kDa
250
180
130
52
####
ns
Rel. pY612-IRS1/IRS1
Rel. pY632-IRS1/IRS1
Rel. pY896-IRS1/IRS1
Rel. pY941-IRS1/IRS1

Figure S3

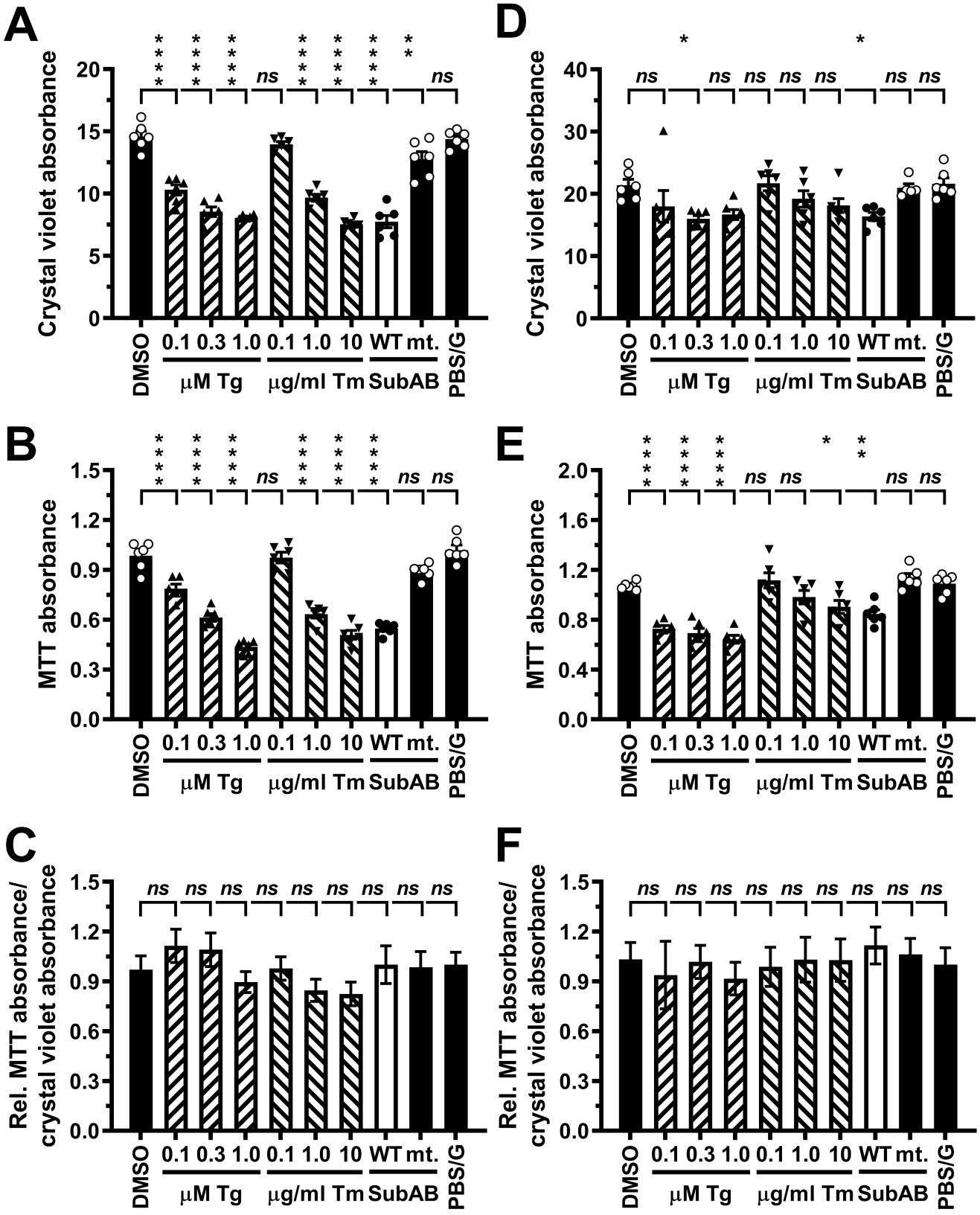
A
Crystal violet absorbance
20
15
10
5
0
DMSO
0.1 0.3 1.0
μM Tg
0.1 1.0 10
μg/ml Tm
WT mt.
SubAB
PBS/G
B
MTT absorbance
1.5
1.2
0.9
0.6
0.3
0.0
C
Rel. MTT absorbance/ crystal violet absorbance
D
40
30
20
10
E
2.0
1.6
0.8
0.4
F
ns
*
**
***
****

Figure S4

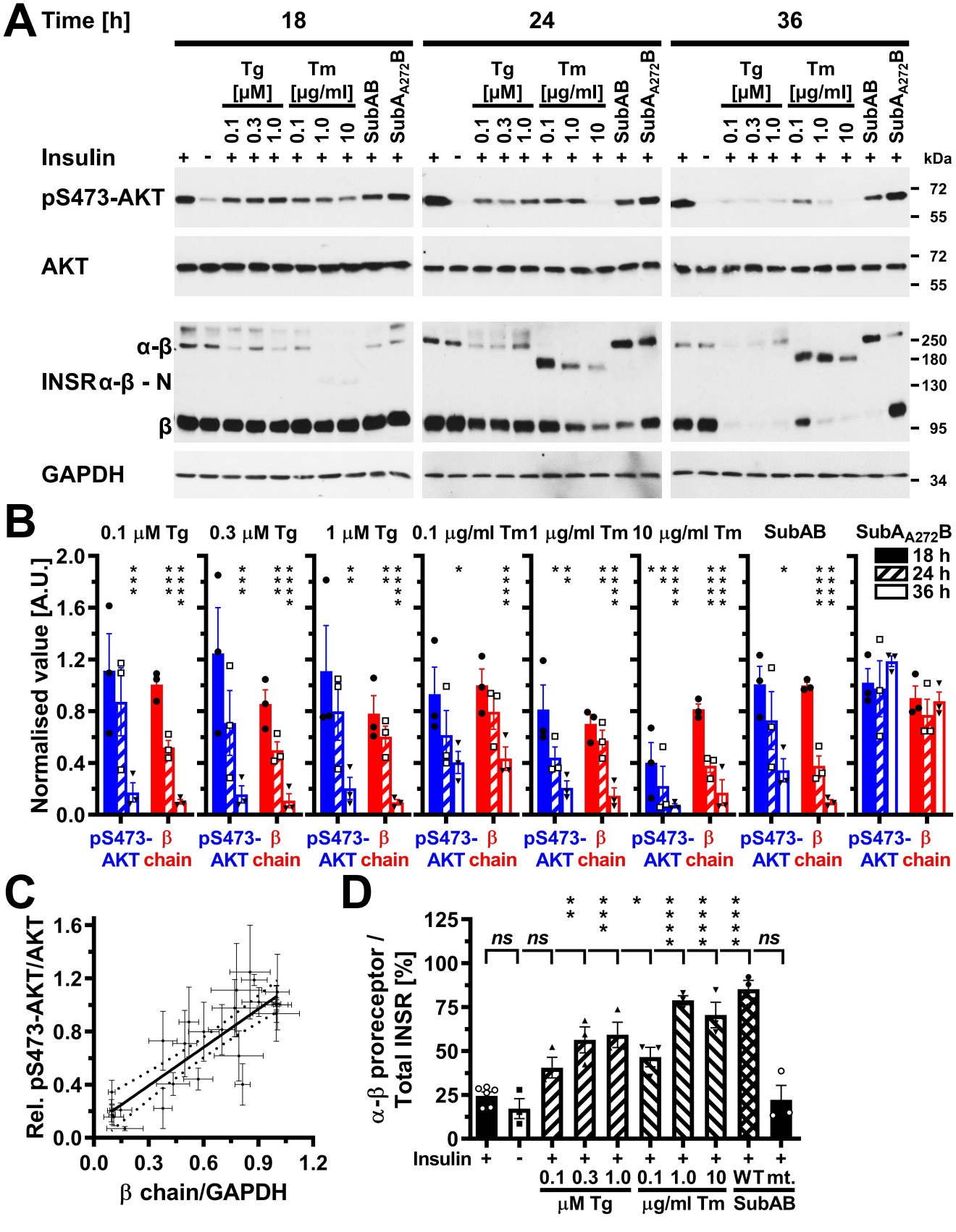
A
Time [h]
18
24
36
Tg [µM]
Tm [µg/ml]
0.1
0.3
1.0
10
SubAB
SubA272B
Insulin
kDa
pS473-AKT
AKT
α-β
INSR α-β - N
β
GAPDH
72
55
250
180
130
95
34
B
0.1 µM Tg
0.3 µM Tg
1 µM Tg
0.1 µg/ml Tm
1 µg/ml Tm
10 µg/ml Tm
SubAB
SubA272B
18 h
24 h
36 h
Normalised value [A.U.]
pS473-AKT
β chain
C
Rel. pS473-AKT/AKT
β chain/GAPDH
D
α-β proreceptor / Total INSR [%]
ns
Insulin
µM Tg
µg/ml Tm
SubAB
WT
mt.

Figure S5

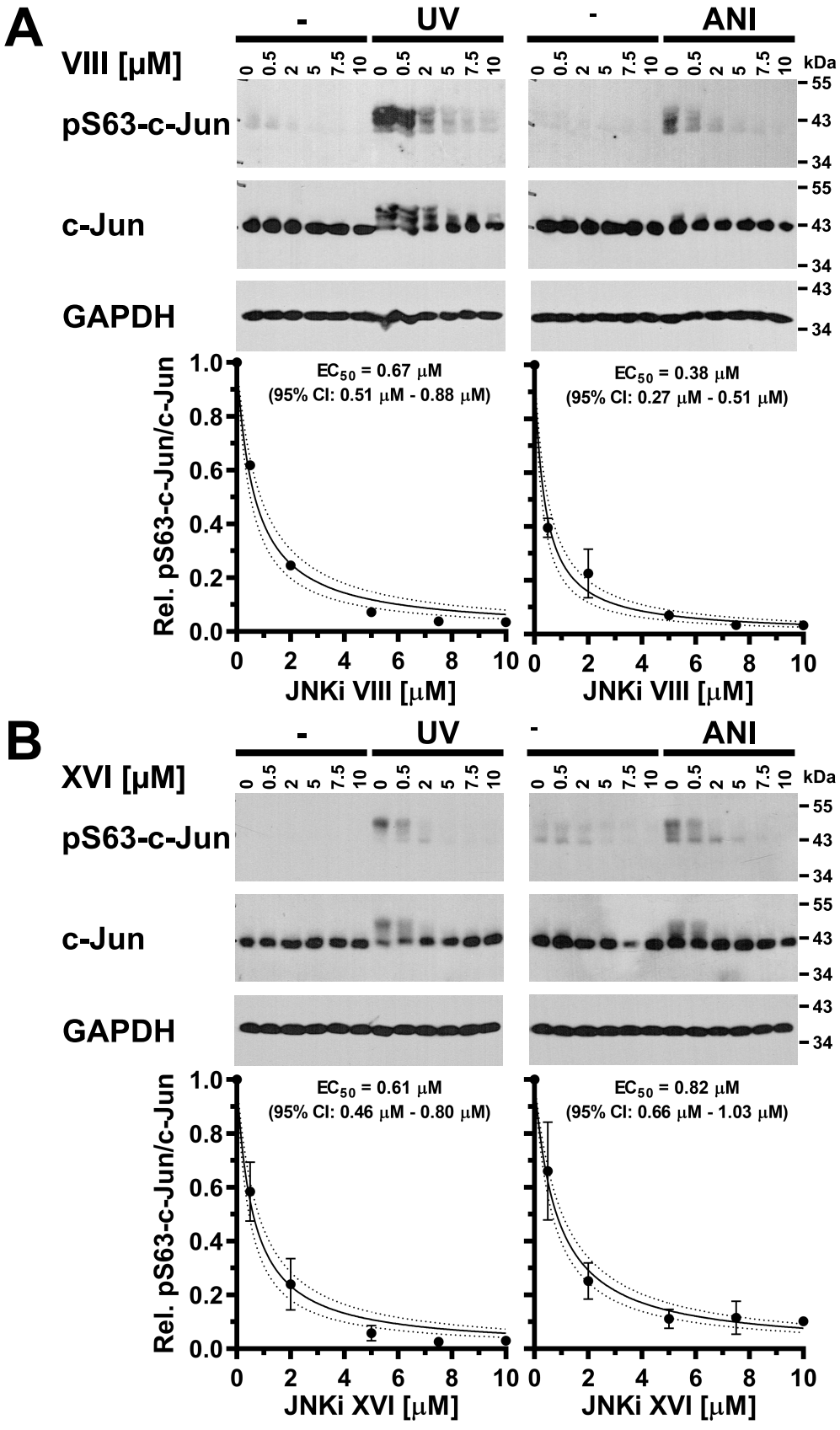
A
-
UV
-
ANI
VIII [µM]
0 0.5 2 5 7.5 10 0 0.5 2 5 7.5 10
0 0.5 2 5 7.5 10 0 0.5 2 5 7.5 10
kDa
pS63-c-Jun
c-Jun
GAPDH
55
43
34
Rel. pS63-c-Jun/c-Jun
EC50 = 0.67 µM
(95% CI: 0.51 µM - 0.88 µM)
EC50 = 0.38 µM
(95% CI: 0.27 µM - 0.51 µM)
JNKi VIII [µM]
B
XVI [µM]
EC50 = 0.61 µM
(95% CI: 0.46 µM - 0.80 µM)
EC50 = 0.82 µM
(95% CI: 0.66 µM - 1.03 µM)
JNKi XVI [µM]

Figure S6

Figure S1. Acute ER stress does not inhibit insulin-dependent AKT activation. (A) Serum starvation does not affect activation of *XBP1* splicing in WT, *ire1α*$^{-/-}$, or *traf2*$^{-/-}$ MEFs, 3T3-F442A cells, C_2C_{12} cells, or Hep G2 cells. Cells were serum-starved for 18 h, where indicated, and then treated with 1 μM thapsigargin for 1 h. (B) 3T3-F442A adipocytes, C_2C_{12} myotubes, and Hep G2 cells were serum-starved for 18 h and treated with the indicated concentrations of thapsigargin, tunicamycin, 1 μg/ml SubAB or $SubA_{A272}B$ during the last 30 min of serum starvation and then stimulated with 100 nM insulin for 15 min, where indicated, in the continued presence of thapsigargin, tunicamycin, SubAB, or $SubA_{A272}B$. Cell lysates were analysed by Western blotting. (C) Quantification of the phosphorylation of AKT on S473. Bars represent standard errors (n = 6 for unstressed, insulin-stimulated cells and n = 3 for all other samples). p values for comparison of ER-stressed samples and samples not stimulated with 100 nM insulin to samples stimulated with 100 nM insulin were calculated by ordinary two-way ANOVA with Dunnett's multiple comparisons test.

Figure S2. Acute ER stress does not inhibit insulin-stimulated phosphorylation of IRS1 at four specific tyrosine phosphorylation sites in 3T3-F442A cells. Tyrosine phosphorylation at (A) Y608, (B) Y628, (C) Y891, and (D) Y935 was analysed by Western blotting. 3T3-F442A cells were serum-starved for 12 h before exposure to 1 μM thapsigargin for 10, 20, or 30 min (left side of figure panels) or to 0.1, 1.0, or 10 μg/ml tunicamycin for 30 min (right side of figure panels), followed by stimulation with the indicated concentrations of insulin for 5 min in the continued presence of thapsigargin or tunicamycin. Bars represent standard errors (n =3 for phosphorylation at Y935, n =4 for phosphorylation at Y608, Y628, and Y891). p values for comparison of effects of thapsigargin or tunicamycin within one insulin concentration and for comparison of effects of different insulin concentrations were calculated by ordinary two-way ANOVA with Tukey's multiple comparisons test. Data for effects of thapsigargin on Y628 phosphorylation of IRS1 were square root-transformed before statistical analyses.

Figure S3. Acute ER stress does not inhibit insulin-stimulated phosphorylation of IRS1 at four specific tyrosine phosphorylation sites in Hep G2 cells. Tyrosine phosphorylation at (A) Y612, (B) Y632, (C) Y896, and (D) Y941 was analysed by Western blotting. Hep G2 cells were

serum-starved for 18 h before exposure to 1 µM thapsigargin for 10, 20, or 30 min (left side of figure panels) or to 0.1, 1.0, or 10 µg/ml tunicamycin for 30 min (right side of figure panels), followed by stimulation with the indicated concentrations of insulin for 5 min in the continued presence of thapsigargin or tunicamycin. Bars represent standard errors (n = 4 for effects of thapsigargin on Y612 phosphorylation, n = 5 for Y632 phosphorylation and effects of thapsigargin on Y896 and Y941 phosphorylation, n = 6 for effects of tunicamycin on Y612 and Y896 phosphorylation, and n = 7 for effects of tunicamycin on Y941 phosphorylation). p values for comparison of effects of thapsigargin or tunicamycin within one insulin concentration and for comparison of effects of different insulin concentrations were calculated by ordinary two-way ANOVA with Tukey's multiple comparisons test. Data for Y896 and Y941 phosphorylation of IRS1 were square root-transformed before statistical analyses.

Figure S4. Prolonged ER stress does not affect viability of (A-C) C_2C_{12} and (D-F) Hep G2 cells. C_2C_{12} and Hep G2 cells were exposed to the indicated ER stressors for 24 h or 36 h, respectively. (A, D) Residual cell staining with crystal violet. (B, E) Determination of cell viability by measurement of the activity of the mitochondrial redox chain with MTT. (C, F) Standardisation of mitochondrial activity measured by reduction of MTT to *N*-[4,5-dimethylthiazol-2-yl]-3,*N*'''-diphenylformazan to cell number determined by crystal violet staining. Bars represent standard errors (n = 6). p values for comparison to the 0.1% (v/v) DMSO control (labelled 'DMSO') were calculated by ordinary one-way ANOVA with Dunnett's multiple comparisons test. Abbreviation: PBS/G – PBS + 50% (v/v) glycerol, added to a final concentration of 0.13% (v/v) to culture medium.

Figure S5. Depletion of insulin receptors correlates with decreased AKT S473 phosphorylation in ER-stressed Hep G2 cells. (A) Serum-starved Hep G2 cells were treated with the indicated concentrations of thapsigargin, tunicamycin, 1 µg/ml SubAB or 1 µg/ml $SubA_{A272}B$ for 18 - 36 h before stimulation with 100 nM insulin for 15 min. Western blots for pS473-AKT, total AKT, the insulin receptor (INSR), and GAPDH. (B) Quantification of the phosphorylation of AKT on S473 ('pS473-AKT') and of the relative abundance of β chains of the insulin receptor ('β chains'). Bars represent standard errors (n = 6 for cells stimulated with 100 nM insulin, n = 3

for all other samples). Phosphorylation of AKT at S473 and the relative abundance of β chains are expressed relative to unstressed cells that were stimulated with 100 nM insulin for 15 min. *p* values for comparison of ER-stressed to unstressed samples were calculated using ordinary two-way ANOVA with Dunnett's multiple comparisons test. (C) Correlation of insulin-stimulated AKT phosphorylation with insulin receptor β chains ($r^2 = 0.74$, two-tailed $p < 0.0001$ for a significantly non-zero slope, and $p > 0.05$ for deviation from linearity calculated by a runs test, $n = 27$). Dotted lines represent the 95% confidence interval of the linear regression line. The relative phosphorylation of AKT at S473 shown in panel B was plotted against the relative abundance of β chains shown in panel B. (D) Quantification of the relative abundance of α-β precursors of the insulin receptor in Hep G2 cells exposed to the indicated concentrations of thapsigargin, tunicamycin, 1 µg/ml SubAB, or $SubA_{A272}B$ for 36 h. Bars represent standard errors ($n = 6$ for unstressed, insulin-stimulated cells and $n = 3$ for all other samples). *p* values for comparison of ER-stressed samples and samples not stimulated with 100 nM insulin to the sample stimulated with 100 nM insulin were calculated using ordinary one-way ANOVA with Dunnett's multiple comparisons test.

Figure S6. JNKi VIII and XVI inhibit phosphorylation of c-Jun at S63 after activation of JNKs in a dose-dependent manner. (A) Dose-response curves for JNKi VIII and (B) JNKi XVI. Hep G2 cells were treated with the indicated concentrations of the JNK inhibitors for 30 min and then stimulated with UV light (400 J/m^2, λ = 254 nm) or treated with 5 µg/ml anisomycin (ANI) for 30 min in the continued presence of the corresponding concentrations of JNKi VIII or XVI. After UV exposure, cells were cultured in the presence of the corresponding concentrations of JNKi VIII or XVI for 30 min. Cell lysates were analysed by Western blotting for pS63-c-Jun, c-Jun, and GAPDH. Relative pS63-c-Jun phosphorylation data were fitted to the equation

$$\text{Rel. pS63-c-Jun phosphorylation} = \frac{1}{1+\frac{[\text{JNKi}]}{EC_{50}}}$$

in GraphPad Prism to calculate EC_{50} values and their 95% confidence intervals (CI).